

The influence of jet geometry on light curves and spectra of GRB afterglows

A.G. Tolstov^{1,2}

¹ Institute for Theoretical and Experimental Physics (ITEP), Bolshaya Cheremushkinskaya, 25, 117218 Moscow, Russia
e-mail: tolstov@mail.itep.ru

² Max Planck Institute for Astrophysics(MPA), Karl-Schwarzschild-Str., 1, 85741 Garching, Germany
e-mail: tolstov@mpa-garching.mpg.de

Received May 26, 2004; accepted November 27, 2004

Abstract. We have performed detailed calculations of spectra and light curves of GRB afterglows assuming that the observed GRBs can have a jet geometry. The calculations are based on an expanding relativistic shock GRB afterglow model where the afterglow is the result of synchrotron radiation of relativistic electrons with power-law energy distribution at the front of external shock being decelerated in a circumstellar medium. To determine the intensity on the radiation surface we solve numerically the full time-, angle-, and frequency-dependent special relativistic transfer equation in the comoving frame using the method of long characteristics.

Key words. gamma rays: bursts – ISM: jets and outflows – radiative transfer

1. Introduction

At the present time we know that gamma-ray bursts (GRBs) are explosive phenomena at cosmological distances. If the emission is isotropic, estimations based on observations give us the values of released energy up to $E_0 \sim 3.4 \times 10^{54}$ ergs for GRB990123, that exceeds the rest energy of a solar mass star (Kulkarni et al. 1999). To reduce this large amount of energy it can be supposed that the GRB emission is highly collimated. May be, the better evidence for jet structure is the achromatic break in light curves (Sari 1999) of the light curves seen in many afterglows, e.g. GRB990123 (Kulkarni et al. 1999) and GRB990510 (Harrison 1999, Stanek 1999). And, finally, spherical symmetry conflicts with linear polarization (Sari 1999) observed for a few afterglows (Covino 1999, Wijers 1999).

Generally, a GRB jet can display an angular structure and can be seen by observer at wide range of viewing angles from the jet axis (Wei & Jin 2003, Granot 2003). For now, however, we consider a jet with uniform angular structure taking into account the effect of equal-arrival-time surface at different angles of observation and show which changes in GRB afterglow are produced in transition from spherical symmetry to jet geometry.

The evolution of the jet and the light curves has been widely investigated (Panaitescu 1999, Kumar 2000), including lateral jet expansion (Salmonson 2003), investigation of the 'structured' jet (Granot 2003), 3D numerical simulations of the jet dynamics (Canizzo 2003) and different angles of observation

(Granot 2002). All these works have not solve accurately transfer equation for the resulting light curves calculations and are based either on simple expressions for local emissivity or focus on power-law branch of the spectrum between the break frequencies or some other simple assumptions on the characteristics of radiation field.

In this paper we present a detailed calculation of spectra and light curves with preliminary numerical solution of special relativistic transfer equation in the comoving frame. We will show that the exact calculation of intensity, depending from the angle to the surface normal, can have an essential influence on the form of the spectra visible to the observer. The exact determination of equitemporal surfaces which is important for explanation of observed luminosity in GRBs and comprehension of their spectral properties (Bianco & Ruffini 1976) is also taken into account in our calculations.

The transfer equation needs to be solved for the accurate calculation of intensity on the surface of radiating structure by integrating the emission along the characteristic through the structure and the following fluxes calculations. The calculation is based on the model where the jet is cut from a spherically symmetric flow. We add two parameters for taking into account a radial jet structure and different values of observer viewing angles. In the next section we discuss our model in more detail, in section 3 we calculate the emission for different values of the parameters and finally we present some discussions and conclusions.

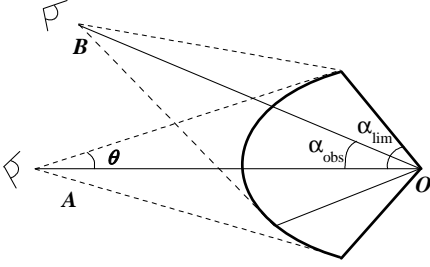


Fig. 1. The part of quasi-ellipsoid from which the photons reach a remote observer. The explosion center is located at the vertex of the jet opening angle α_{lim} . The jet is observed under the angle α_{obs} between the jet symmetry axis and the direction towards the observer.

2. Physical Model

Our jet geometry investigation is based on the numerical solution of the problem in the spherically-symmetric case. To take into account jet geometry first we fix the direction towards the observer in the case of spherical symmetry. Because of the high shock velocity light at a certain time reaches the observer from the ellipsoidal structure, the part of which can be seen in Fig. 1. To construct the jet we cut the cone with axis being the direction towards the observer A and the angle α_{lim} , forming jet opening angle. The sight of observer A in this case coincides with jet axis. To consider the jet under different values of viewing angle we add angle α_{obs} between the observer B and the jet axis. This approach gives us the possibility to consider some jet effects without using specific hydrodynamics code and more complicated transfer equation.

Let us consider the model we have used for numerical calculations of spectra and light curves in the case of spherical symmetry (Tolstov & Blinnikov 2003).

In general, the transfer and hydrodynamic equations constitute a combined system of equations. In our problem, however, we solve them separately. To determine the variables of the medium we use a self-similar solution for a relativistic shock for an ultrarelativistic gas in the case of the conservation of total shell energy (Blandford & McKee 1976). The solution describes the explosion with a fixed amount of energy E_0 and propagation of a relativistic shock through a uniform cold medium.

$$p = \frac{1}{3}e = \frac{2}{3}w_1\Gamma^2\chi^{-17/12}; \quad \gamma^2 = \frac{1}{2}\Gamma^2\chi^{-1}; \quad n\gamma = 2n_1\Gamma^2\chi^{-7/4},$$

where

$$\Gamma^2 \propto t^{-3}; \quad \chi = [1 + 8\Gamma^2](1 - r/t).$$

Above, Γ is the Lorentz factor of the shock front, γ , p , e , n - the Lorentz factor, pressure, energy and density of the shocked fluid, measured in the local rest frame of fluid, respectively, and n_1 is density of the external medium.

For accurate calculation we should know also the electron energy spectrum and the magnetic field strength. Here for local emissivity calculation we use the conventional assumptions from relativistic electrons (e.g. Sari 1999). We assume being based on standard fireball shock model (Zhang 2003) that the electrons have a power-law distribution and that their total energy behind the shock front accounts for ϵ_e of the internal energy:

$$N(\gamma_e) = K_0\gamma_e^{-p}; \quad \gamma_e \geq \gamma_{\text{min},0} = \frac{\epsilon_e e_0}{n_0 m_e c^2},$$

where m_e is the electron rest mass and $K_0 = (p-1)n_0\gamma_{\text{min},0}^{p-1}$.

The magnetic field is parameterized by the quantity ϵ_B , which is equal to the fraction of the internal energy contained in the magnetic field $B^2 = 8\pi\epsilon_B e$. The magnetic field is randomly oriented and decreases with time due to adiabatic expansion of the shell.

As the electrons pass through the shock they begin to lose the energy through adiabatic cooling determined by the solution of Blandford & McKee (1976). This process is well described in detail by Granot & Sari (2002).

Here we present only the basic formulas for synchrotron radiation used in our calculation. The spectral power of a single electron averaged over the pitch angle is:

$$P(\omega) = \frac{3^{5/2}}{8\pi} \frac{P_{\text{sy}}}{\omega_0} F\left(\frac{\omega}{\omega_c}\right),$$

where

$$P_{\text{sy}} = \frac{1}{6\pi} \sigma_{\text{Th}} c B^2 (\gamma_e^2 - 1); \quad \omega_c = \frac{3\pi}{8} \frac{eB}{m_e c} \gamma_e^2,$$

and $F(u)$ - a standard synchrotron radiation function (Rybicki 1979). The synchrotron absorption coefficient is specified by the formula:

$$\chi = \frac{1}{8\pi m_e v^2} \int_{\gamma_{\text{min}}}^{\gamma_{\text{max}}} d\gamma \frac{N(\gamma)}{\gamma^2} \frac{d}{d\gamma} \left(\gamma^2 P(\omega, \gamma) \right)$$

To determine the intensity on the radiation surface we solve numerically the full time-, angle-, and frequency-dependent relativistic transfer equation in the comoving frame using the method of long characteristics up to the values of Lorentz-factor $\gamma \sim 1000$.

After the calculation of intensity the flux can be determined:

$$F_{0,\text{obs}} = \frac{2\pi}{D^2} \int_{\mu_{0,\text{min}}}^1 \mu R^2 I(r(\mu_0), v_0 \left(\frac{v}{v_0}\right), \cos \delta(\cos \delta_0)) \left(\frac{v_0}{v}\right)^3 d\mu_0,$$

where subscript 0 is related to the observer frame, D is the distance to observer, $p = R/D$. μ_{min} - cosine of the maximum angle visible to the observer.

To sum up, the observer afterglow spectra and light curves depend on the the hydrodynamic evolution, the radiation processes, the distance to the observer and the two parameters we have used for taking into account jet structure: the jet opening angle α_{lim} and the viewing angle α_{obs} .

In our calculation for solving the problem in the case of spherical symmetry we have used the following parameters:

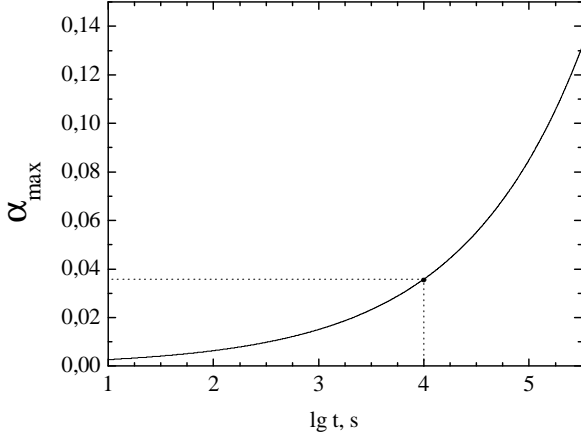


Fig. 2. The angle visible to observer from emitting structure increases with time. Time is measured in the observer frame of reference. For the $t = 10^4$ s it is shown that there is no reasons to increase the jet opening angle more that 0.037.

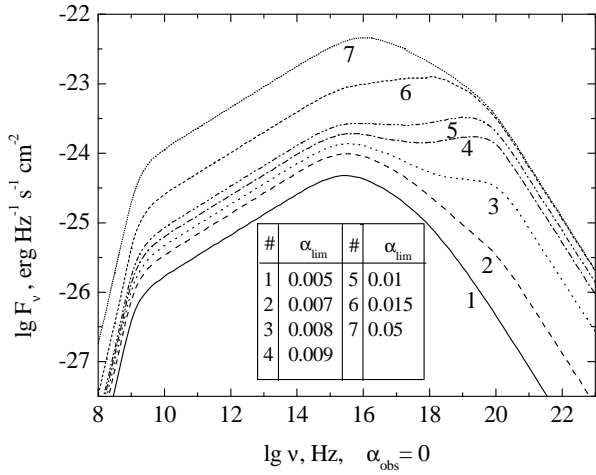


Fig. 3. Instantaneous afterglow spectra at time $t = 10^4$ s and observational angle $\alpha_{obs} = 0$ for different values of limitation angle α_{lim} .

$E_0 = 10^{53}$ ergs, $n_1 = 1 \text{ cm}^{-3}$, $\epsilon_e = 0.5$, $\epsilon_B = 0.1$, $p = 2.5$, $D = 10^{27}$ cm. In the next section we consider the results of the jet geometry influence on spectra and light curves varying α_{lim} and α_{obs} .

3. Results of the numerical calculation

As the shell from which the light reaches the observer moves towards the observer, the angle of the structure visible to the observer increases with time. This dependence is presented in Fig. 2, where α is the angle between the direction to the observer and the line connecting the center of the symmetry with the point on the surface that is still visible to the observer. There

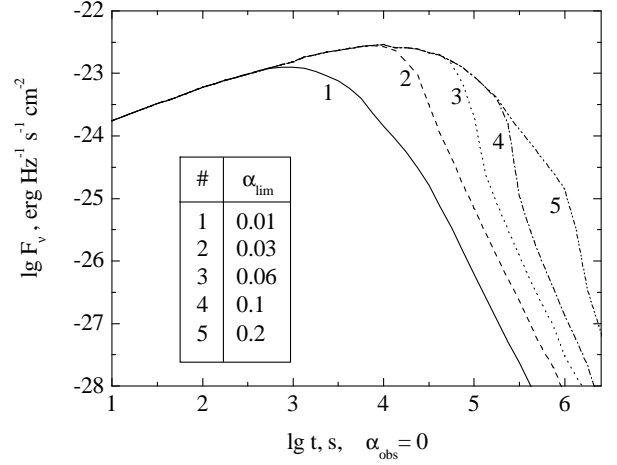


Fig. 4. Afterglow light curves at frequency $\nu = 5 \times 10^{14}$ Hz and observational angle $\alpha_{obs} = 0$ for different values of limitation angle α_{lim} .

is the following relationship between the real observation angle θ and α has :

$$\cos \theta = \frac{1 - \mu p(\mu)}{[1 + p^2(\mu) - 2p(\mu)\mu]^{1/2}},$$

where $\mu = \cos \alpha$, $p = R(t_{obs})/D$, $t_{obs} = t_{obs}(\mu, p, D)$, D - distance from the center of the burst to the observer, and time in the burst frame of reference t is connected with the time in the observer frame of reference t_{obs} by the formula:

$$t_{obs} = t + \frac{D(1 - [1 + p^2(\mu) - 2p(\mu)\mu]^{1/2}) + R_0}{c} \approx \\ \approx t + \frac{R_0 - R(t_{obs})}{c} \quad (p \ll 1)$$

if we suppose that the initial time of observation corresponds to the initial time of the burst ($t_0 = t_{0,obs} + D/c$) and initial radius of the burst structure is R_0 .

Now if we fix the time of observation by the value, say, of $t'_{obs} = 10^4 c$, there is no reason to increase the value of limitation angle in our jet structure for more than $\alpha'_{lim} = 0.037$ (Fig. 2), because this does not produce any effect on the resulting spectra and light curves as if they are considered from the non-limited structure.

In Fig. 3 and Fig. 4 we can see the calculated spectra and light curves at zero observational angle and at different values of limitation angle.

The changed form of the spectra, having at some values of limitation angle two peak fluxes, is the consequence of the ring intensity structure on the radiative surface (Tolstov & Blinnikov 2003).

If we look at the ring structure we see that than more the light frequency than closer the maximum of brightness to the edge of the image.

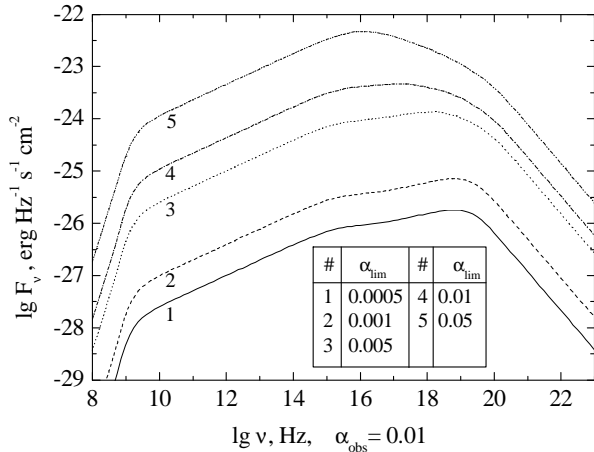


Fig. 5. Instantaneous afterglow spectra at time $t = 10^4$ s and observational angle $\alpha_{obs} = 0.01$ for different values of limitation angle α_{lim} .

The flux from the observed image can be calculated by the formula

$$F_\nu = 2\pi \int_{\cos\theta_{max}}^1 I(\cos\theta, r, \nu) \cos\theta d\cos\theta$$

where θ is the angle between the point on the radiating surface and the center of the structure (see Fig. 1), θ_{max} corresponds to the edge of the image. In the absence of jet limitation angle the flux is monotonically decrease in increasing light frequency at the right part of the spectrum. In the presence of limitation angle some maximums of intensity at lower frequencies are excluded from the flux integral and it gives at higher frequencies flux value compatible to that one at lower frequencies.

The light curves do not show this effect just having "jet breaks" due to the limitation angle. This results from decreasing of the radiation arrived to the observer from the shock limited by α_{lim} . Larger the value of α_{lim} , less radiation at some frequencies gets towards the observer. Of order of days at $\alpha_{lim} = 0.2$ we can see the break typical for some observed optical afterglows (Zhang & Meszaros 2003).

In Fig. 5 and Fig. 6 we present the calculated spectra and light curves at the observational angle $\alpha_{obs} = 0.01$. At small values of limitation angles we can see also the changes in spectra but for the light curves we did not have this effect. Some of the presented light curves are cut at early moments of time. This is the consequence of solving transfer equation only up to the Lorentz-factor value $\gamma = 1000$. At larger value of Lorentz-factor we suppose that the matter is not radiative and if at $\alpha_{obs} = 0$ this effect is not revealed that at $\alpha_{obs} = 0.01$ some of the characteristics start at Lorentz-factor value $\gamma \geq 1000$.

4. Conclusions

It is widely believed that GRBs are born in jet geometry. In this case the resulting afterglow radiation becomes highly collimated. The numerical calculations of light curves in these

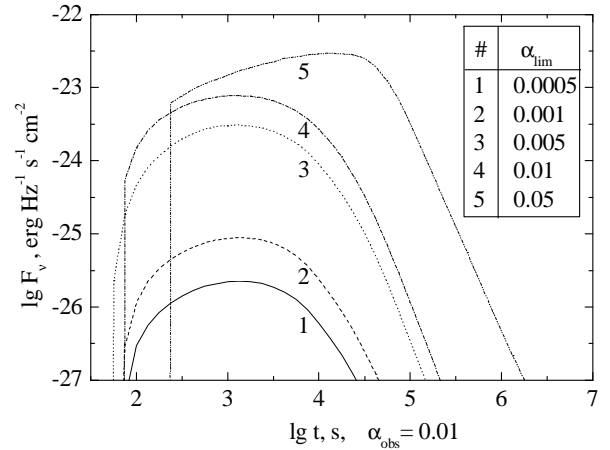


Fig. 6. Afterglow light curves at frequency $\nu = 5 \times 10^{14}$ Hz and observational angle $\alpha_{obs} = 0.01$ for different values of limitation angle α_{lim} .

models (Granot 2003, Salmonson 2003) are based on some assumptions for intensity on the propagating shock front. The shape of the local spectral emissivity is approximated as a broken power-law with some typical breaks corresponding to synchrotron radiation. As we can see from our results the spectra can have some peculiarities and the shapes different from power-law as in direct view to the jet as at some angle to the jet axis.

Of course, our consideration does not take into account some effects of jet model and the exact numerical calculations should be at least two-dimensional to allow lateral expansion and angular structure of the jet.

Nevertheless we would like to point out that the accurate calculation of intensity using relativistic transfer equation can have an influence on the shape of spectra and light curves of GRB afterglow. Constructing more precise model using the exact numerical calculations can help to explain the peculiarities of GRB afterglow and shed some light on the nature of GRB phenomenon.

Acknowledgements. I am grateful to S.I. Blinnikov for posing the problem and for valuable discussions. Also I wish to convey my sincerest thanks to H. Spruit for the kind hospitality at the Max-Planck Institute for Astrophysics, under the auspices of which this work was performed. The work in Russia is partly supported by RBRF grant 02-02-16500.

References

- Blandford R.D., McKee C.F., Phys. Fluids, **19**, 1130 (1976)
- Bianco C.L. & Ruffini R., astro-ph/0403379, (2004)
- Canizzo J.K., Gehrels N., Vishniac E.T., astro-ph/0310113, (2003)
- Covino S., et al., A&A **348**, L1, (1999)
- Granot J., Sari R., ApJ **568**, 820, (2001)
- Granot J., Panaitescu A., Kumar P., Woosley S.E., ApJ **570**, L61, (2002)
- Granot J., Kumar P., ApJ **591**, 1086, (2003)
- Harrison F.A, Bloom J.S., Frail D.A., et al., ApJ **121**, 523, (1999)

- Kulkarni S.R., Djorgovski S.G., Odewhan S.C., et al. *Nature* **389**, 398, (1999)
- Kumar P., Panaitescu A., *ApJ* **541**, L9, (2000)
- Panaitescu A., Meszaros P., *ApJ* **526**, 707, (1999)
- Rybicki G.B., Lightman A.P., *Radiative processes in astrophysics* (Wiley, New York, 1979)
- Salmonson J.D., *ApJ* **592**, 1002, (2003)
- Sari R., Piran T., Halpern G.P., *ApJ* **519**, L17, (1999a)
- Sari R., *ApJ* **524**, L43, (1999b)
- Sari R., Piran T., Narayan R., *ApJ* **489**, L33, (1999c)
- Stanek K.Z., Garnavich P.M., Kaluzny J., et al., *ApJ* **522**, L39, (1999)
- Tolstov A.G., Blinnikov S.I., *AstL* **29**, 403 (2003)
- Wei D.M., Jin Z.P., *A&A* **400**, 415, (2003)
- Wijers R.A.M.J., et al., *ApJ* **874**, 571, (1999)
- Zhang B., Meszaros P., astro-ph/0311321, (2003)

